PHYSICAL REVIEW A VOLUME 31, NUMBER 4 APRIL 1985

Spectral shapes of Mössbauer absorption and incoherent neutron scattering from harmonically bound nuclei in Brownian motion: Applications to macromolecular systems

I. Nowik, E. R. Bauminger, S. G. Cohen,* and S. Ofer*
Racah Institute of Physics, The Hebrew University, 91904 Jerusalem, Israel

(Received 10 October 1984)

The Mössbauer resonance absorption line in solids is of narrow, natural width. In viscous liquids the linewidth is broadened by diffusion. In many biological systems—whole cells, membranes, or proteins—at temperatures above the freezing point of the internal water, a superposition of broad and narrow lines is observed. Here, the Mössbauer spectral shapes expected in this new "phase" of proteinic matter are calculated. The calculation is based on the assumption that the unfrozen conformational degrees of freedom of the macromolecules can be described in terms of damped harmonic oscillators acted upon by random forces. The known classical correlation functions for harmonically bound particles in Brownian motion are utilized to calculate the Mössbauer spectra. The theory predicts the following: a spectrum which can be approximated by a superposition of a narrow and a broad line; and a sharp decrease in the total resonance absorption as a function of temperature and asymmetric quadrupole doublets in ^{57}Fe spectra, even when the Debye-Waller factor is isotropic but the damping frequencies are anisotropic. The presented formulas, with only minor changes, are also applicable to the description of neutron quasielastic scattering from systems in which nuclei diffuse in restricted geometries: bound diffusion on surfaces, lamellar systems, ionic polymers, biopolymers, and membranes. Finally, calculated spectra are compared to recent experimental Mössbauer spectra, and the agreement is outstanding. The spectral shape of particles participating in both bound translational and free rotational diffusion is also calculated.

I. INTRODUCTION

Recent studies of the Mössbauer absorption in biological systems such as proteins and membranes and in polymers[1–9] reveal unusual spectra, different from those observed in ordinary solids or viscous liquids. The spectra can be described as composed of a narrow line, as in solids, and a broad line, as that observed in liquids. Quasielastic incoherent neutron scattering from nuclei in bound geometries display similar spectra.[10,11] In the present paper we apply the theory of damped harmonic oscillators in Brownian motion developed by Uhlenbeck and Ornstein[12] to calculate the expected Mössbauer absorption spectra and neutron scattering spectra in such systems.[13–16] Comparison is made to other formulas developed for Mössbauer and neutron spectroscopy of nuclei performing bound diffusion in solids and liquids.[10,13,15,17–19] The present calculation predicts Mössbauer spectra which can be looked upon, to a good approximation, as composed of a narrow and broad lines with total intensity strongly temperature dependent. When the diffusion is anisotropic it predicts a generalized Karyagin-Goldanskii effect,[20] even when the Debye-Waller factor is isotropic. The calculated Mössbauer spectra are compared to various experimental observations and the agreement is very satisfactory. In the Appendix the spectral shape obtained in spherical particles participating in both bound translational and free rotational diffusion is calculated in detail.

II. THEORY

A. Dynamics of a harmonically bound particle

The general formula for a Mössbauer spectrum in the classical limit is given by[10,21]

$$I(\omega)=\frac{1}{2\pi}\int_{-\infty}^{\infty}dt\,\exp[-i(\omega-\omega_0)t-\tfrac{1}{2}\Gamma|t|]\times\int_{\mathbf{r}}d\mathbf{r}_0d\mathbf{r}\,G(\mathbf{r},\mathbf{r}_0,t)\times\exp[i\mathbf{k}\cdot(\mathbf{r}-\mathbf{r}_0)]p(\mathbf{r}_0)\ . \qquad (1)$$

Here Γ is the natural width of the Mössbauer line, $\mathbf{k}$ is the γ-ray wave vector, and $G(\mathbf{r},\mathbf{r}_0,t)$ is the probability that at time t the nucleus will be at $\mathbf{r}$ if at time zero it was at $\mathbf{r}_0$. $p(\mathbf{r})$ is the stationary probability of the particle being at $\mathbf{r}$, which equals $G(\mathbf{r},\mathbf{r}',\infty)$ and is of course independent of $\mathbf{r}'$.

A particle of mass m bound to a center by a harmonic force $-mw^2\mathbf{r}$, damped by a frictional force $-m\beta\dot{\mathbf{r}}$, and acted upon by random forces $\mathbf{F}(t)$ will follow the equation of motion

$$m\ddot{\mathbf{r}}+m\beta\dot{\mathbf{r}}+mw^2\mathbf{r}=\mathbf{F}(t)\ . \qquad (2)$$

In the case of one-dimensional motion, Uhlenbeck and Ornstein[12] have derived general formulas for $G(x,x_0,t)$. Their formula for the overdamped case, which seems to be relevant in biological systems, and generalized to three dimensions, yields

$$G(\mathbf{r},\mathbf{r}_0,t)=\left[\frac{\alpha}{2\pi D(1-e^{-2\alpha t})}\right]^{3/2}\times\exp\left[-\frac{\alpha(\mathbf{r}-\mathbf{r}_0e^{-\alpha t})^2}{2D(1-e^{-2\alpha t})}\right]. \tag{3}$$

Here $\alpha=w^2/\beta$ is the ratio of the harmonic and damping force constants and $D=k_BT/m\beta$ is the diffusion constant. The mean-square displacement after a long period of time is given by $\langle x^2\rangle=k_BT/mw^2=D/\alpha$. The parameter α is also $1/\tau_c$ where τ_c is the relaxation time of the ensemble average of x,[12] $\langle x\rangle_t=x_0\exp(-t/\tau_c)$ and $\langle x^2\rangle_t=k_BT/mw^2+(x_0^2-k_BT/mw^2)\exp(-2t/\tau_c)$. Thus the two parameters $\langle x^2\rangle$ and τ_c^{-1} characterize completely the statistical averages of the microscopic motion of the particle.

Inserting Eq. (2) into Eq. (1) and performing the Fourier transform of $G(\mathbf{r},\mathbf{r}_0,t)$ and then the integration on $\mathbf{r}_0$ gives the final formula for the spectrum, as a function of angular frequency;[14]

$$I(\omega)=\frac{1}{2\pi}\int_{-\infty}^{\infty}dt\exp\left[-i(\omega-\omega_0)t-\tfrac{1}{2}\Gamma|t|-\frac{k^2D}{\alpha}(1-e^{-\alpha|t|})\right]. \tag{4}$$

We have used Eq. (4) to compute the absorption spectra as a function of the parameters $\alpha=1/\tau_c$ and $D=\alpha\langle x^2\rangle$. Examples are shown in Fig. 1 for a fixed value of D and a range of values of α. These spectra are normalized for the sake of display to constant maximum resonance absorption. We observe from Eq. (4) that for a very small value of α (free particle), a Lorentzian spectrum of half-width $\Gamma/2+k^2D$, as expected for a freely diffusing particle,[21] is obtained. For large α, $\alpha/\Gamma=w^2/\beta\Gamma\gg 1$, though keeping still within the overdamped limit $w\ll\beta$, $I(\omega)$ becomes a Lorentzian of natural width Γ. At intermediate values of α the spectra have the peculiar shapes shown in Fig. 1. Equation (4) can be presented by an infinite sum of Lorentzian lines which converges very fast. Expanding $\exp(k^2\langle x^2\rangle e^{-\alpha t})$ in a power series[9,15] yields

$$I(\omega)=\exp(-k^2\langle x^2\rangle)\times\sum_{n=0}^{\infty}\frac{(k^2\langle x^2\rangle)^n}{n!}\,\frac{(\frac{1}{2}\Gamma+n\alpha)/\pi}{(\frac{1}{2}\Gamma+n\alpha)^2+(\omega-\omega_0)^2}. \tag{5}$$

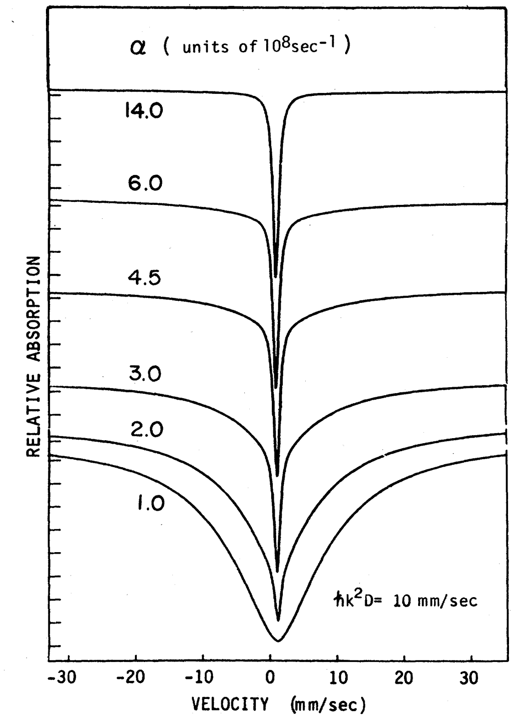

FIG. 1. Mössbauer spectra of harmonically bound particles containing ^{57}Fe in Brownian motion as a function of the parameter $\alpha=w^2/\beta$, for a fixed value of the diffusion constant $D=1.4\times10^{-9}$ cm^2/sec corresponding to a value of $\hbar k^2D$ equal to 10 mm/sec in units of the Doppler velocity ($\hbar\Gamma$ was fixed at a value of 0.75 mm/sec).

In Fig. 2 the intensities of the first seven Lorentzian lines in the sum of Eq. (5) are displayed as a function of $k^2\langle x^2\rangle$. In the approximation of a single narrow line ($n=0$) and one broad line, the width of the broad line can be calculated by a harmonic average;

$$\frac{2\alpha}{\Gamma_{\text{eff}}}=\frac{1}{\exp(k^2\langle x^2\rangle)-1}\sum_{n=1}^{\infty}\frac{(k^2\langle x^2\rangle)^n}{n!}\,\frac{1}{(\Gamma/2\alpha+n)}. \tag{6}$$

Γ_{eff} was calculated for various $k^2\langle x^2\rangle$ values and is shown in Fig. 3. Thus one can use a two-line approxima-

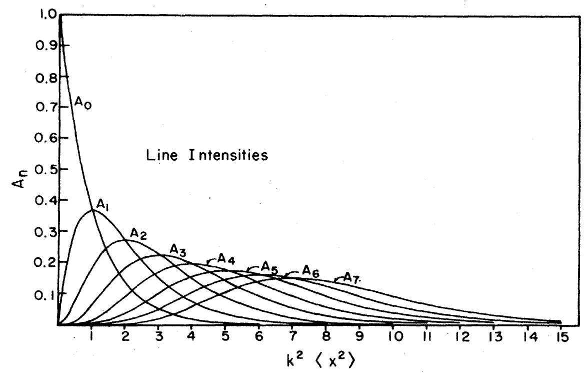

FIG. 2. Relative intensities of the Lorentzian lines of width $\Gamma+2n\alpha$ appearing in Eq. (5), as a function of $k^2\langle x^2\rangle$.

tion, derive $k^2\langle x^2\rangle$ from the relative intensities of the two lines, and then obtain α from Fig. 3.

We have obtained Eq. (4) for the overdamped case. For the sake of generality, we quote the form of the absorption spectrum for arbitrary w and β:

$$I(\omega)=\frac{1}{2\pi}\int_{-\infty}^{\infty} dt\,\exp[-i(\omega-\omega_0)t]\exp(-\tfrac{1}{2}\Gamma\,|\,t\,|\,)\times\exp\{-k^2\langle x^2\rangle[1-\phi(t)]\}\;, \tag{7}$$

where

$$\phi(t)=\begin{cases} e^{-\beta|t|/2}\left[\cos(w_1t)+\dfrac{\beta}{2w_1}\sin(w_1t)\right], & w_1^2=w^2-\left[\dfrac{\beta}{2}\right]^2>0\\ e^{-\beta|t|/2}\left[1+\dfrac{\beta}{2}t\right], & w=\beta/2\\ e^{-\beta|t|/2}\left[\cosh(w't)+\dfrac{\beta}{2w'}\sinh(w't)\right], & (w')^2=\left[\dfrac{\beta}{2}\right]^2-w^2>0\;. \end{cases}$$

We have seen a closed-form expression for $I(\omega)$ in the overdamped limit, both in an integral and in a sum-of-Lorentzians form. The extreme underdamped case can also be expressed in a convenient form as a sum of Lorentzians. In the extreme underdamped case the expression for $\phi(t)$ can be approximated by

$$\phi(t)=e^{-\beta|t|/2}\cos(wt)\;.$$

A power-series expansion of $\exp[k^2\langle x^2\rangle e^{-\beta|t|/2}\cos(wt)]$ yields

$$I(\omega)=\frac{1}{2\pi}e^{-k^2\langle x^2\rangle}\times\sum_{n=0}^{\infty}\frac{(k^2\langle x^2\rangle)^n}{n!}\times\left[\frac{(\Gamma+n\beta)/2}{[(\Gamma+n\beta)/2]^2+(\omega-\omega_0-nw)^2}+\frac{(\Gamma+n\beta)/2}{[(\Gamma+n\beta)/2]^2+(\omega-\omega_0+nw)^2}\right]\;. \tag{8}$$

We observe that in the overdamped case the spectrum is composed of Lorentzian lines of width $\Gamma+2n\alpha$ at ω_0, whereas in the underdamped case one observes sideband lines at $\omega_0\pm nw$ of width $\Gamma+n\beta$. The intensities in both cases are the same.

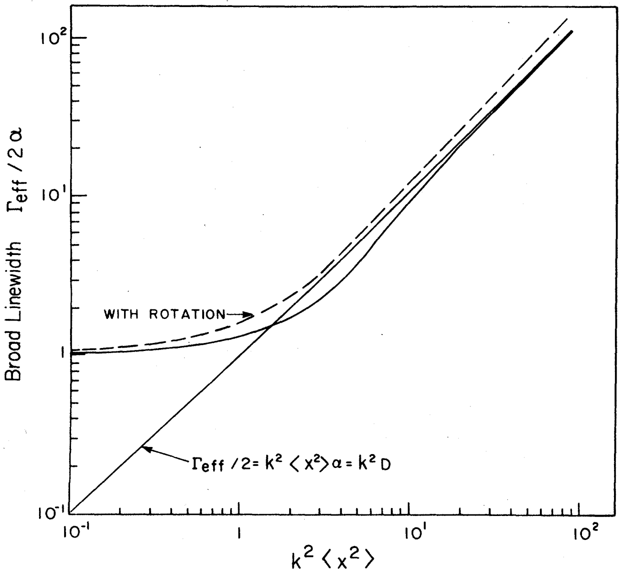

FIG. 3. The effective linewidth of the broad line, in the two-Lorentzian-lines approximation of Eq. (4) or Eq. (5), as a function of $k^2\langle x^2\rangle$.

The model described above can be generalized to treat anisotropic diffusive motions which might be relevant in particular systems, as, e.g., in single-crystal proteins or oriented membranes. For the anisotropic overdamped harmonic oscillator, with independent motions along the three axes, Eq. (4) becomes generalized to the form

$$I(\omega)=\frac{1}{2\pi}\int_{-\infty}^{\infty} dt\,\exp[-i(\omega-\omega_0)t-\tfrac{1}{2}\Gamma\,|\,t\,|\,-k_x^2\langle x^2\rangle(1-e^{-\alpha_x|t|})-k_y^2\langle y^2\rangle(1-e^{-\alpha_y|t|})-k_z^2\langle z^2\rangle(1-e^{-\alpha_z|t|})]\;, \tag{9}$$

where $\alpha_x=w_x^2/\beta_x$, and similarly for α_y and α_z.

The line shape, including narrow and wide components, will then depend on the angle of incidence of the γ rays.

In polycrystalline proteins or unoriented membranes, in those cases where there are appreciable quadrupole hyperfine interactions, one might expect a generalized Karyagin-Goldanskii[20] effect, the observed line shape being a sum of different lines corresponding to the various transitions between the substates of the hyperfine structure. Thus in a powder sample, the spectral shape of a nuclear transition between quantum numbers M_1 and M_2, with $M_1-M_2=\Delta M$ will be given by

$$I(\omega)=\frac{1}{8\pi^2}\int_\phi\int_\theta\int_{-\infty}^{\infty}dt\,\exp\{-i(\omega-\omega_0)t-\tfrac{1}{2}\Gamma|t|-k^2\cos^2\theta\langle x^2\rangle(1-e^{-\alpha_x|t|}) -k^2\sin^2\theta[\cos^2\phi\langle y^2\rangle(1-e^{-\alpha_y|t|})+\sin^2\phi\langle z^2\rangle(1-e^{-\alpha_z|t|})]\} \times f(\Delta M,\theta)\sin\theta\,d\theta\,d\phi\ , \tag{10}$$

where $f(\Delta M,\theta)$ for the transition in ^{57}Fe, is given by $f(0,\theta)=\frac{3}{2}\sin^2\theta$ and $f(\pm1,\theta)=\frac{3}{4}(1+\cos^2\theta)$. For axial symmetry $(\langle z^2\rangle=\langle y^2\rangle,\ \alpha_y=\alpha_z)$ we obtain for the two ^{57}Fe quadrupole lines the spectral shapes $(\eta=\cos\theta)$

$$I_s(\omega)=\frac{1}{2\pi}\int_{-\infty}^{\infty}dt\int_0^1\exp[-i(\omega-\omega_0)t-\tfrac{1}{2}\Gamma|t|-k^2\langle x^2\rangle(1-e^{-\alpha_x|t|})\eta^2 -k^2\langle y^2\rangle(1-e^{-\alpha_y|t|})(1-\eta^2)]f_s(\eta)d\eta\ , \tag{11}$$

where $f_1(\eta)=\frac{3}{4}(1+\eta^2)$ and $f_2(\eta)=\frac{3}{4}(\frac{5}{3}-\eta^2)$. Spectra calculated using Eq. (11) for various α_x and α_y values are shown in Fig. 4. The asymmetry in the spectra is observable even when $\langle x^2\rangle=\langle y^2\rangle$.

The theoretical treatment given above assumed oscillators of a single frequency (Einstein model). We can extend the treatment to a general distribution of normal frequencies and damping frequencies (Debye model).

If a γ-ray-absorbing nucleus is bound to a macroscopic entity, such as a macromolecule, its motion $\mathbf{r}$ can be expanded in the molecular normal-mode coordinates q_l with $l=1,2,\ldots,N$. If the wave vector of the γ ray is $\mathbf{k}=k\epsilon$, we can write

$$(\mathbf{k}\cdot\mathbf{r})=k(\epsilon\cdot\mathbf{r})=k\sum_l a_l q_l\ . \tag{12}$$

If we assume that all normal-mode coordinates follow the harmonic damped motion given by Eq. (2),[13] and if in all cases the overdamped limit is applicable (this requirement can be relaxed, as will be discussed later), then, as all normal modes are statistically uncorrelated, we obtain

$$G(\mathbf{r},\mathbf{r}_0,t)d\mathbf{r}=\prod_l g(q_l,q_{0l},t)dq_l\ , \tag{13}$$

where q_{0l} are normal mode coordinates at time zero,

$$g(q_l,q_{0l},t) =\frac{\exp\{-(q_l-q_{0l}e^{-\alpha_l t})^2/[2\langle q_l^2\rangle(1-e^{-2\alpha_l t})]\}}{[2\pi\langle q_l^2\rangle(1-e^{-2\alpha_l t})]^{1/2}} \tag{14}$$

and

$$\alpha_l=w_l^2/\beta_l\ .$$

Performing the double Fourier transform on q_l and q_{0l} we get

$$I(\omega)=\frac{1}{2\pi}\int_{-\infty}^{\infty}\exp\left[-i(\omega-\omega_0)t-\tfrac{1}{2}\Gamma|t| -k^2\sum_l a_l^2\langle q_l^2\rangle(1-e^{-\alpha_l|t|})\right]dt\ . \tag{15}$$

If out of the N modes there are m modes for which $\alpha_j\gg\Gamma$ $(j=1,2,\ldots,m)$, namely, $w_j^2/\beta_j\gg\Gamma$ or β_j is relatively small yet still $\beta_j\gg\Gamma$, we obtain that within the finite range of experimental observation, $|\omega_{\max}-\omega_0|<500\Gamma$,

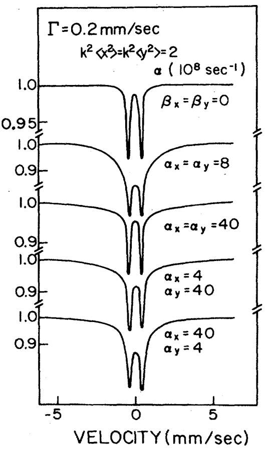

FIG. 4. Mössbauer spectra of harmonically bound particles acted upon by axially symmetric anisotropic damping forces.

$$I_{\text{expt}}(\omega)\approx\left[\exp^{-k^2}\left[\sum_{j=1}^{m}a_j^2\langle q_j^2\rangle\right]\right]\frac{1}{2\pi}\int_{-\infty}^{\infty}\exp\left[-i(\omega-\omega_0)t-\tfrac{1}{2}\Gamma|t|-k^2\sum_{l\,(\neq j)}a_l^2\langle q_l^2\rangle(1-e^{-\alpha_l|t|})\right]dt \tag{16}$$

and

$$f_{\text{tot}}=\int_{\omega_0-500\Gamma}^{\omega_0+500\Gamma}I_{\text{expt}}(\omega)d\omega$$
$$\approx\exp\left[-k^2\sum_{j=1}^{m}a_j^2\langle q_j^2\rangle\right]=\exp(-k^2\langle x_f^2\rangle)\,, \tag{17}$$

where $\langle x_f^2\rangle$ refers to fast fluctuation rates, $\alpha_j \gg \Gamma$.

Thus again the experimental spectrum consists of a superposition of a narrow and broad line, the narrow line of width Γ of relative intensity

$$f_{\text{nar}}=\exp\left[-k^2\sum_{l\,(\neq j)}a_l^2\langle q_l^2\rangle\right]$$

and the broad line of relative intensity $1-f_{\text{nar}}$. The broad line is composed of many lines each of which has a half-width $\Gamma/2+\sum_{l\,(\neq j)}n_l\alpha_l$ and intensity

$$\prod_{l\,(\neq j)}[(k^2a_l^2\langle q_l^2\rangle)^{n_l}/n_l!]f_{\text{nar}}\,,$$

where $\{n_l\}$ are series of integers, $\sum_l n_l=n$, $n=1,2,3,4,\ldots$ The total intensity is given by f_{tot}. Thus the absolute intensity of the narrow line is $f_{\text{tot}}f_{\text{nar}}$ and that of the broad line is $f_{\text{tot}}(1-f_{\text{nar}})$. In biological systems at the "phase transition" between the solid phase and "viscous liquid" phase, the extra degrees of freedom of the molecular motions melt, become active, and contribute both to the appearance of a broad line and to a sharp decrease in the total resonance absorption f_{tot}.[5]

It is worth mentioning that for very high α values assumed for the m modes, namely large w and small β, the underdamped limit may be reached. However, since $w>\beta\gg\Gamma$ Eq. (8) shows that only the $n=0$ line will be observable and thus all previous conclusions are still valid.

The theoretical treatment given in the present paper is similar to those given by Knapp *et al.*[15] and Shaitan and Rubin[16] for Mössbauer spectroscopy and by Rahman *et al.*[13] for neutron scattering. However, the present treatment is characterized by the following. (a) It presents the final formula in a closed form. (b) It treats the problem in three dimensions and this enables the introduction of anisotropic binding and damping forces in a very simple way. (c) It presents a way to analyze a Mössbauer spectrum in terms of only two lines and yet obtain all the physical information which would have been obtained by applying the exact formula, Eq. (4). (d) It treats the general distribution of restoring and damping frequencies in a scheme which does not require additional parameters in analyzing the experimental spectra, except for the mean-square displacement of the fast fluctuations, $\langle x_f^2\rangle$.

B. Comparison with dynamics of diffusion in a cage

We have concluded that the relative intensity of the narrow line f_n is given by $\exp(-k^2\langle x^2\rangle)$. It is worthwhile to compare this expression to the value given within a model of discrete jumps of the ion among N equivalent sites (diffusion within a cage) which also predicts narrow and broad lines.[17–19] The recoil-free fraction of the absorption line of natural width is given in this model[17,18] as

$$f=f_0\left|\frac{1}{N}\sum_n e^{i\mathbf{k}\cdot\mathbf{R}_n}\right|^2$$
$$=f_0\frac{1}{N}\sum_n\frac{1}{N}\sum_m e^{i\mathbf{k}\cdot(\mathbf{R}_n-\mathbf{R}_m)}\,, \tag{18}$$

where $\mathbf{R}_n$ are the coordinates of the nth atom.

In a polycrystalline sample the orientation of $\mathbf{k}$ relative to $\mathbf{R}_{nm}=\mathbf{R}_n-\mathbf{R}_m$ is random and can be averaged out to yield

$$f=f_0\frac{1}{N}\sum_n\left[\frac{1}{N}\sum_m\frac{\sin(kR_{nm})}{kR_{nm}}\right]. \tag{19}$$

This formula yields, for the case of $N=2$,

$$f=f_0\left[\tfrac{1}{2}+\tfrac{1}{2}\frac{\sin(kd)}{kd}\right],\quad R_0^2=\tfrac{1}{4}d^2\,; \tag{20a}$$

for $N=4$ (tetrahedron),

$$f=\tfrac{1}{4}f_0\left[1+3\frac{\sin(kd)}{kd}\right],\quad R_0^2=\tfrac{3}{8}d^2\,; \tag{20b}$$

for $N=6$ (octahedron),

$$f=\tfrac{1}{6}f_0\left[1+\frac{\sin(\sqrt{2}kd)}{\sqrt{2}kd}+4\frac{\sin(kd)}{kd}\right],$$
$$R_0^2=\tfrac{1}{2}d^2\,; \tag{20c}$$

for $N=8$ (cube),

$$f=\tfrac{1}{8}f_0(1+3Z_1+3Z_2+Z_3)\,,$$
$$Z_l=\frac{\sin(kd\sqrt{l}\,)}{kd\sqrt{l}},\quad R_0^2=\tfrac{3}{4}d^2\,. \tag{20d}$$

Here d is the shortest "jump" distance and R_0 is the distance of each site to the center.

If we now allow $N\to\infty$, with all N points equivalent as in the previous cases, and located on a spherical surface of radius R_0, then the sum in Eq. (19) becomes

$$\frac{f}{f_0}=\int_0^{2R_0}\frac{\sin(kR)}{kR}\frac{1}{2R_0^2}R\,dR=\frac{\sin^2(kR_0)}{(kR_0)^2}\,. \tag{21}$$

The average value for the square jumping distance is $\langle R^2\rangle=2R_0^2$.

According to Eq. (21), R_0 of about 0.4 Å for the 14.4-keV transition of ^{57}Fe makes the narrow absorption line invisible ($<1\%$). This result is different from that obtained assuming a finite number N. For a finite number

N, even when $\langle R^2\rangle$ is very large, a finite intensity $1/N$ stays with the absorption line of natural width. In the model based on the overdamped harmonic oscillator, the recoil-free fraction for atoms oscillating around a center within distance R_0 would be given by $\exp(-\frac{1}{3}k^2R_0^2)$ which coincides with Eq. (21) only for low values of kR_0.

Within the above model of jumps among N equivalent sites the Mössbauer spectrum consists of many broad lines which together appear as a single broad line of half-width $\gamma/2=\Gamma/2+\Delta/2$ where, as before, Γ is the natural linewidth. The extra width Δ will now be given approximately by the general "diffusion-jump" models,[21,22] $\Delta=2\lambda[1-g(\mathbf{k})]$, where λ is the jumping rate and $g(\mathbf{k})$ is the Fourier transform of $g(\mathbf{r})$,[22] the probability to jump a distance $\mathbf{r}$. In our case, if we assume that the probability to jump to any point is the same, the probability to jump a distance between R and $R+dR$ is just the number of points in that region. Thus we obtain for $g(\mathbf{k})$ the same formula as that for f/f_0 and may write

$$\Delta=2\lambda(1-f/f_0)\ . \tag{22}$$

The diffusion constant is defined by the formula $D=\frac{1}{6}\lambda\langle R^2\rangle$. For $kR_0\ll1$, $\Delta=2k^2D$, which is consistent with the ordinary diffusion broadening formula. In this case, where $\langle R^2\rangle=2R_0^2$ and $R_0=3\langle x_0^2\rangle$, we obtain $D=\lambda\langle x_0^2\rangle$ and thus λ in the jump model coincides with α of the harmonically bound diffusion model.[16]

C. Application to incoherent neutron scattering

The same formulas presenting the Mössbauer spectra also represent the spectral function for scattered neutrons. The only differences are (a) the natural width Γ can be dropped, (b) ω_0 is zero, and (c) instead of the convolution with the source line in the Mössbauer case, a convolution with the experimental energy resolution function has to be performed. The present formulas can thus be used successfully for representing neutron scattering spectra from diffusing nuclei in bound geometries. It is of interest to make a comparison of the predictions of Eq. (4) with those of Eq. (33) of Ref. 10, which treats the effects of bound diffusion in a sphere of radius R on neutron scattering spectra. Of special interest is the linewidth of the broad line as a function of the momentum transfer $\mathbf{k}$. Within the present model, the half-width of the broad line, Fig. 3, is k independent for low values of k and equals $\alpha=D/\langle x^2\rangle=3D/\langle r^2\rangle$. The model of bound diffusion in a sphere yields at low k a broad line of half-width $4.333D/R^2$ (Fig. 2 in Ref. 10). Considering that $\langle r^2\rangle$ in our model represents a Gaussian average of the particles' motion amplitude, and R in Ref. 10 represents the largest displacement of the particle, the two formulas are not much different at all. At high k values both models yield a broad line with half-width k^2D.

We conclude that neutron spectroscopy of nuclei in bound diffusion can be treated by Eq. (4) or Eq. (5), with advantages of Eq. (4) for clarity of behavior in extreme cases and in anisotropic cases and of Eq. (5) for computing purposes. The sum converges very fast in comparison to the slowly converging sum of Eq. 33 in Ref. 10.

III. EXPERIMENTAL RESULTS

In Fig. 5 we present typical ^{57}Fe absorption spectra obtained near room temperature in four different biological systems which are

(a) iron storage material in packed cells of chick embryo fibroblasts,[8]

(b) membrane-bound iron storage material from *Mycoplasma capricolum*,[14]

(c) membrane-bound iron storage in packed cells of *Escherichia coli*,[6] and

(d) crystals of deoxy-myoglobin (deoxyMb) highly enriched in ^{57}Fe.[5]

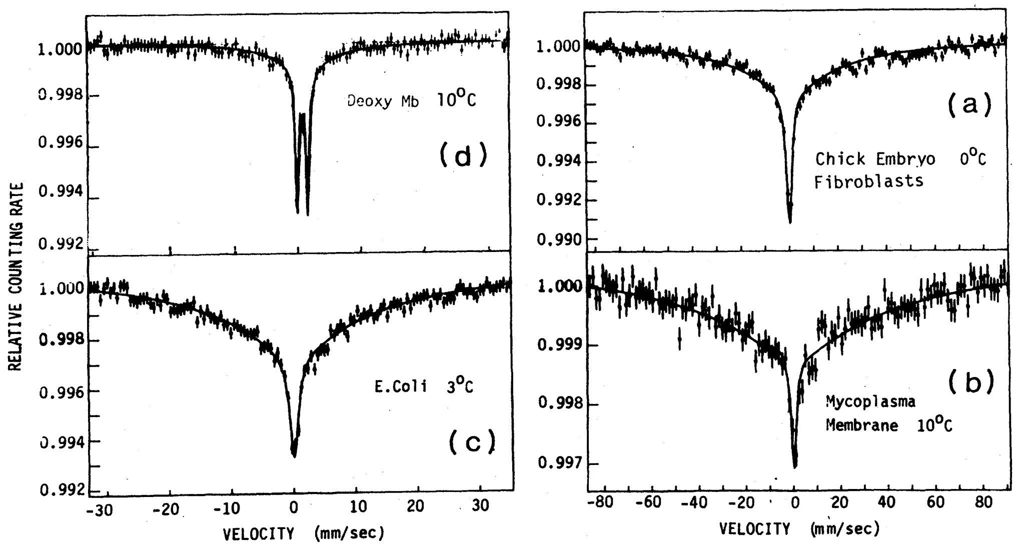

FIG. 5. Mössbauer absorption spectra in various biological systems containing ^{57}Fe. The solid curves are theoretical least-squares fits using Eq. (4). The parameters D (in units of 10^{-10} cm/sec) and α (in units of 10^8 sec^{-1}), are respectively, (a) 40, 10; (b) 87, 13; (c) 26, 5; and (d) 4.3, 2.5.

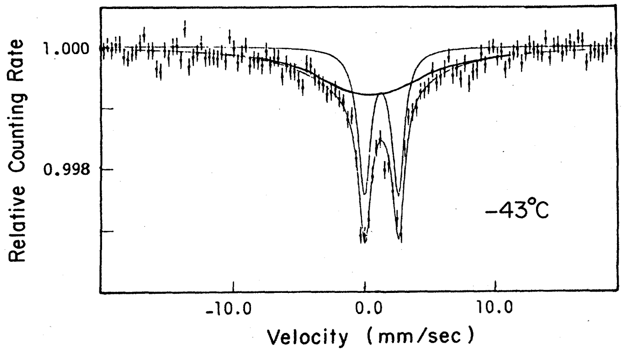

FIG. 6. Mössbauer spectrum of ^{57}Fe in divalent iron Nafion at 230 K. The inner lines show the decomposition of the spectrum into the elastic narrow doublet and the quasielastic broad line. (Nafion is the trade name for perfluorosulfonate membranes developed by DuPond.)

In cases (a), (b), and (c) the iron is in the form of inorganic aggregates of size less than 50 Å bound strongly to the membranes. In (d) each protein molecule contains a single iron atom which is part of the heme group, bound within the protein.

A least-squares fit of Eq. (4) to the experimental data for deoxyMb crystals [Fig. 5(d)] at 283 K yields $D=4.3\times10^{-10}$ cm$^2s^{-1}$, $\langle x^2\rangle=1.7\times10^{-2}$ Å^2, and $\alpha=2.5\times10^{8}$ sec^{-1} or $\tau_c=4\times10^{-9}$ sec. The diffusive motions of Fe in deoxyMb are large-scale internal motions of structures internal to the protein of which the iron atom is a part.[5] Assuming, therefore, that m is of the order of the mass of the protein (molecular weight 17 000), we obtain $\beta\sim3\times10^{15}$ s^{-1} and $w\sim9\times10^{11}$ s^{-1}. We thus see that indeed, $w\ll\beta$ and $\beta t\gg1$ (t is of the order of 10^{-7} sec—the lifetime of the ^{57}Fe excited state), as is assumed in deriving Eq. (4). The parameters derived in the three other biological systems displayed in Fig. 5 are given in the figure captions. In all cases consistently better fits were obtained using Eq. (4) compared to fits to the sum of a narrow and a wide Lorentzian line, in accord with simple diffusion-jump models. Another example of the phenomena discussed is observed in Fig. 6 which displays Mössbauer spectra of iron nuclei performing bound diffusion in a polymer.[7]

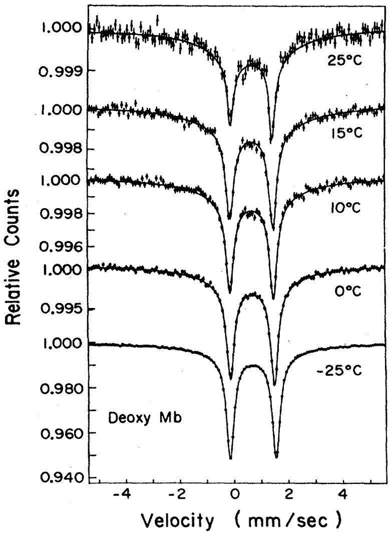

FIG. 7. Mössbauer spectra of Fe in deoxy-myoglobin which display anisotropic harmonically bound motion. The spectra were fitted by Eq. (9) assuming axially symmetric mean-square displacement ($\langle x_{\parallel}^2\rangle$ and $\langle x_{\perp}^2\rangle$) and isotropic β.

In Fig. 7 we display the experimental spectra of deoxyMb (Ref. 23) which definitely exhibit an asymmetric shape at temperatures above the freezing point of the internal water, yet none at temperatures below this freezing point, 220 K. Thus one is tempted to fit these spectra with the formula of Eq. (9) with anisotropy in the mean-square deviation. Such least-squares fits are shown in Fig. 7.

IV. CONCLUSIONS

Many aspects of the expected spectra from nuclei performing bound diffusion are not very sensitive to the exact dynamical model for the kind of motion. All theories predict a narrow, elastic line with additional broad quasielastic lines. The relative intensity of the narrow line and the width of the broad line are numerically similar in all theories, though given by different mathematical expressions. The unique properties of the present model are that it considers many modes of motion, as well as anisotropic motion, and yields a closed-form formula which can be easily calculated in extreme limits and easily calculated by computer. Only with very accurate experimental spectra will one be able to distinguish between the relative validity of different dynamical models.

ACKNOWLEDGMENTS

This work was supported in part by the Basic Research Foundation, Israel Academy of Sciences and Humanities.

APPENDIX: SPECTRA FROM NUCLEI IN PARTICLES PERFORMING BOTH BOUND TRANSLATIONAL AND FREE ROTATIONAL DIFFUSION

In cases where the diffusing bound particle is composed of many molecules, as in the case of a rigid macroscopic particle, rotational diffusion may influence the Mössbauer or scattered neutron spectral shapes. The case of bound translational diffusion was treated in great detail in the present paper; the case of free rotational diffusion was treated in detail elsewhere.[24] For a nucleus at a distance r from the center of mass of the particle, the intermediate scattering function, for a γ ray of wave vector $\mathbf{k}$, or neutron wave-vector change $\mathbf{k}$, is given by

$$F_{\rm rot}(r,\mathbf{k},t)=\sum_{l=0}^{\infty}(2l+1)j_l^2(kr)e^{-l(l+1)D_{\rm rot}t}\,. \qquad (A1)$$

Here $j_l(x)$ is a spherical Bessel function and $D_{\rm rot}$ is the rotational diffusion constant.

Considering the translational and rotational motion as uncorrelated, we can calculate the spectral shape for the composed motion. The total intermediate scattering function is given by [see Eq. (4)]

$$F_{\text{tot}}(r,\mathbf{k},t)=F_{\text{rot}}(r,\mathbf{k},t)\exp[-k^2\langle x^2\rangle(1-e^{-\alpha t})] \; . \tag{A2}$$

Performing the expansion as in Eq. (5) we obtain that the final spectral function is given by a double infinite sum of Lorentzian lines:

$$\begin{aligned} I(r,\omega)&=\frac{1}{2\pi}\int_{-\infty}^{\infty} e^{-i(\omega-\omega_0)-\Gamma|t|/2}F_{\text{tot}}(r,\mathbf{k},t)dt \\ &=\sum_{l=0}^{\infty}\sum_{n=0}^{\infty}\frac{a_{nl}(r)\Gamma_{nl}/2\pi}{(\Gamma_{nl}/2)^2+(\omega-\omega_0)^2} \; , \end{aligned} \tag{A3}$$

where

$$\Gamma_{nl}/2=\Gamma/2+n\alpha+l(l+1)D_{\text{rot}}$$

and

$$a_{nl}=\exp(-k^2\langle x^2\rangle)\frac{(k^2\langle x^2\rangle)^n}{n!}(2l+1)j_l^2(kr) \; .$$

In practice we have to average the spectrum over all values of r in which the nuclei are located. For a spherical particle of radius R with a homogeneous density of nuclei, the spectrum of Eq. (A3) will be given by

$$I(\omega=\frac{3}{R^3}\int_0^R I(r,\omega)r^2dr \; .$$

Thus the spectrum is still the same sum of Lorentzians as in Eq. (A3) except that now the intensities are given by

$$\begin{aligned} A_{nl}(R)&=\frac{3}{R^3}\int_0^R a_{nl}(r)r^2dr \\ &=\tfrac{3}{2}e^{-k^2\langle x^2\rangle}\frac{(k^2\langle x^2\rangle)^n}{n!}(2l+1) \\ &\quad\times[j_l^2(kR)+j_{l-1}^2(kR) \\ &\qquad-\frac{2l+1}{kR}j_l(kR)j_{l-1}(kR)] \; . \end{aligned} \tag{A4}$$

In the simple case of a homogeneous spherical particle the spectrum is completely characterized by three parameters; the radius R, the mean-square deviation $\langle x^2\rangle$, and the diffusion constant D (where $\alpha=D/\langle x^2\rangle$ and $D_{\text{rot}}=\frac{3}{4}D/R^2$).

For $k^2\langle x^2\rangle>5$ the translational diffusion behaves as unbounded diffusion, Fig. 3, and the intermediate spectral function can be taken as $\exp(-k^2Dt)$. Thus the total spectrum will be given by

$$I(r,\omega)=\sum_{l=0}^{\infty}\frac{a_l(r)\Gamma_l/2\pi}{(\Gamma_l/2)^2+(\omega-\omega_0)^2} \; , \tag{A5}$$

where

$$a_l(r)=(2l+1)j_l^2(kr)$$

and

$$\Gamma_l/2=\Gamma/2+k^2D+l(l+1)D_{\text{rot}} \; .$$

Again, in the case of a homogeneous spherical particle after averaging over r, one obtains the spectrum of Eq. (A5) with intensities

$$\begin{aligned} A_l(R)&=\frac{3}{R^3}\int_0^R a_l(r)r^2dr \\ &=\tfrac{3}{2}(2l+1)[j_l^2(kR)+j_{l-1}^2(kR) \\ &\qquad-\frac{2l+1}{kR}j_l(kR)j_{l-1}(kR)] \; . \end{aligned}$$

Since the narrowest line in Eq. (A5) is of width $\Gamma+2k^2D$ and since generally $\Gamma \ll k^2D$ and, at least in the Mössbauer case, $D_{\text{rot}} \ll k^2D$ also, we expect that Eq. (A5) can be reproduced by a single Lorentzian line of a width slightly larger than $2k^2D$. In the case of a homogeneous spherical particle, where $D_{\text{rot}}=\frac{3}{4}D/R^2$, one can calculate the effective width of the spectrum given by Eq. (A5) by equating

$$\frac{\Gamma_{\text{eff}}/2\pi}{(\Gamma_{\text{eff}}/2)^2+(\omega-\omega_0)^2}=\sum_{l=0}^{\infty}\frac{A_l(R)\Gamma_l/2\pi}{(\Gamma_l/2)^2+(\omega-\omega_0)^2} \; . \tag{A6}$$

At $\omega=\omega_0$, considering $k^2D \gg \Gamma/2$, we obtain

$$\frac{2k^2D}{\Gamma_{\text{eff}}(R)}=\sum_{l=0}^{\infty}\frac{A_l(R)}{1+\frac{3}{4}l(l+1)/k^2R^2} \; .$$

In Fig. 8, Γ_{eff} (in units of $2k^2D$) is displayed as a function of kR. For $kR \sim 3$, the value of Γ_{eff} is in full saturation, and equals $1.271\times 2k^2D$. Thus for a macroscopic particle, even the size of a small molecule ($R\sim 5$ Å), the Mössbauer spectrum will be affected by rotational diffusion only to the extent of broadening the translational diffusion line by 20—30%.

In the general case of a sphere performing bound translational and free rotational diffusion, one can represent Eq. (A3) by a superposition of an effective narrow line, the $n=0$ line broadened by rotation, and a broad line, $n\geq 1$, also broadened by the rotations. The effective

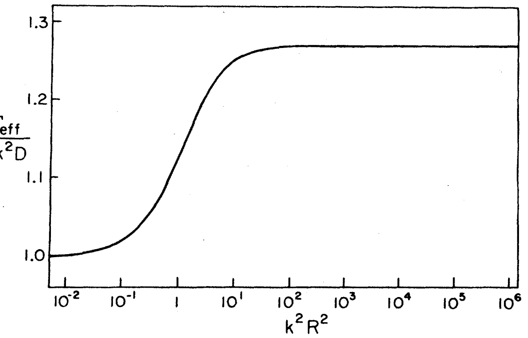

FIG. 8. The effective width of the spectral shape from nuclei in a spherical particle of radius R performing free translational and rotational diffusion.

width of these two lines can be calculated by the harmonic averages

$$\frac{1}{\Gamma_{\mathrm{nar}}}=\sum_{l=0}^{\infty}\frac{A_{0l}}{\Gamma_{0l}}$$

and

$$\frac{1}{\Gamma_{\mathrm{brod}}}=\sum_{n=1}^{\infty}\sum_{l=0}^{\infty}\frac{A_{nl}}{\Gamma_{nl}}\ .$$

These were calculated as functions of $k^2\langle x^2\rangle$ for $k^2R^2>1000$. In Fig. 9 Γ_{nar} is given in units of Γ as a function of $2k^2D/\Gamma$. Γ_{brod} is shown in Fig. 3, in units of 2α. We observe that the effect of rotation on the broad line is about the same for all $k^2\langle x^2\rangle$ values. In a recent paper[25] we have applied the formulas discussed in this appendix to analyze the spectra of iron in magnetic particles located in bacteria.

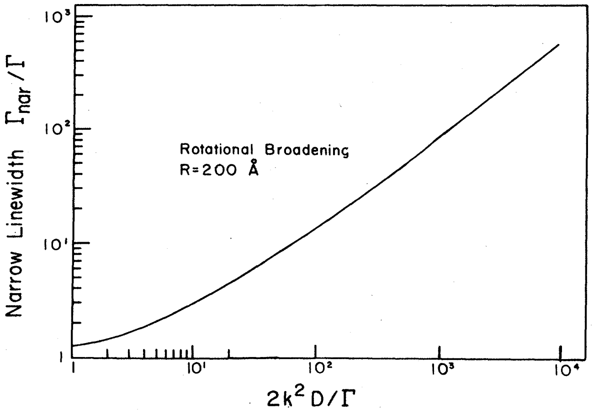

FIG. 9. The line broadening of the $n=0$ line of Eq. (A3) for spherical particles of radius R ($kR>10$) as a function of the diffusion constant.

---

*Deceased.

[1] S. G. Cohen, E. R. Bauminger, I. Nowik, S. Ofer, and J. Yariv, Phys. Rev. Lett. **46**, 1244 (1981).

[2] S. G. Cohen, E. R. Bauminger, I. Nowik, S. Ofer, and J. Yariv, in *Biomolecular Stereodynamics,* edited by R. H. Sarma (Adenine, New York, 1981), Vol. II, p. 299.

[3] E. R. Bauminger, S. G. Cohen, I. Nowik, S. Ofer, and J. Yariv, in *Proceedings of the 1981 International Conference on Applications of the Mössbauer Effect, Jaipur, India,* edited by V. G. Bhide (Indian National Academy, New Delhi, 1982).

[4] K. H. Mayo, F. Parak, and R. L. Mössbauer, Phys. Lett. **82A**, 468 (1981).

[5] E. R. Bauminger, S. G. Cohen, I. Nowik, S. Ofer, and J. Yariv, Proc. Natl. Acad. Sci. (U.S.) **80**, 736 (1983).

[6] E. R. Bauminger, S. G. Cohen, E. Giberman, I. Nowik, S. Ofer, J. Yariv, M. M. Werber, and M. Mevarech, J. Phys. (Paris) Colloq. **37**, C6-227 (1976).

[7] E. R. Bauminger, I. Nowik, S. Ofer, and C. Virguin-Heitner, Polymer (to be published).

[8] E. R. Bauminger, S. G. Cohen, S. Ofer, and U. Bachrach, Biochim. Biophys. Acta **720**, 133 (1982).

[9] F. Parak, E. W. Knapp, and D. Kucheida, J. Mol. Biol. **161**, 177 (1982).

[10] F. Volino and A. J. Dianoux, Mol. Phys. **41**, 271 (1980).

[11] F. Volino, M. Pineri, A. J. Dianoux, and A. Degeyer, J. Polym. Sci., Polym. Phys. Ed. **20**, 481 (1982).

[12] G. E. Uhlenbeck and L. S. Ornstein, Phys. Rev. **36**, 823 (1930).

[13] A. Rahman, K. S. Singwi, and A. Sjölander, Phys. Rev. **126**, 997 (1962).

[14] I. Nowik, S. G. Cohen, E. R. Bauminger, and S. Ofer, Phys. Rev. Lett. **50**, 1528 (1983).

[15] E. W. Knapp, E. W. Fischer, and F. Parak, J. Chem. Phys. **78**, 4701 (1983).

[16] K. V. Shaitan and A. B. Rubin, Biofizika **25**, 796 (1980).

[17] A. Bläsius, R. S. Preston, and U. Gonser, Z. Phys. Chem. **115**, 187 (1979).

[18] W. Petry, G. Vogl, and W. Mansel, Phys. Rev. Lett. **45**, 1862 (1980); W. Petry and G. Vogl, Z. Phys. B **45**, 207 (1982).

[19] S. Dattagupta, Solid State Commun. **24**, 19 (1977).

[20] V. I. Goldanskii and E. F. Makarov, in *Chemical Applications of Mössbauer Spectroscopy,* edited by V. I. Goldanskii and R. H. Herber (Academic, New York, 1968), p. 102.

[21] K. S. Singwi and A. Sjölander, Phys. Rev. **120**, 1093 (1960).

[22] S. Dattagupta, Phys. Rev. B **14**, 1329 (1976); **12**, 47 (1975).

[23] E. R. Bauminger, S. G. Cohen, I. Nowik, S. Ofer, and J. Yariv, Hyperfine Interact. **15/16**, 881 (1983).

[24] *Quasielastic Neutron Scattering for the Investigation of Diffusive Motions in Solids and Liquids,* Vol. 64 of *Springer Tracts in Modern Physics,* edited by T. Springer (Springer, Berlin, 1972), p. 64.

[25] S. Ofer, I. Nowik, E. R. Bauminger, G. C. Papaefthymiou, R. B. Frankel, and R. B. Blakemore, Biophys. J. **46**, 57 (1984).